A Simple Algorithm for High-Accuracy Maximum Power Point Calculation of Photovoltaic Systems

Orlando Trejo and Adelmo Ortiz-Conde

***Abstract*—We present a simple algorithm to perform fast and high-accuracy calculations of the maximum power point of illuminated photovoltaic panels, based on fixed-point iteration. This simple and rigorous procedure presents a fast convergence for a large range of initial values. Our algorithm is illustrated by applying it to measurements of photovoltaic modules with seven different technologies. The possibility of using the first iterations as a practical approximate solution is also considered.**

***Index Terms*—Fixed-point iteration, Lambert W function, maximum power point (MPP), photovoltaic (PV) panels, solar cell.**

I. Introduction

THE current of illuminated photovoltaic (PV) panels and solar cells are customarily described by the single diode model [1]–[10], which contains a diode, a current source, a series resistance, and a parallel conductance. This simple model with only five parameters presents a reasonable accuracy. In some particular cases, more sophisticated models are used, as for example—the double diode model with seven parameters [11]–[12], the triple diode model with nine parameters [13], and the alternative multiexponential model [14].

The evaluation of the maximum power point (MPP) (i.e., the maximum voltage $V_{\rm mpp}$ and the corresponding maximum current $I_{\rm mpp}$) is a crucial research topic in PV systems and its applications [15], [16]. This issue has received significant attention and several articles have been published to that effect for the single diode model [6]–[9]. Most of them represent approximate solutions [6], [9], which are valid in some particular cases, and the others are rigorous numerical calculations [7], [8], [17], [18]. In general, the approximate analytical expressions are faster but less accurate than the rigorous iterative solutions. To the best of our knowledge, there is not a rigorous analytical solution to calculate the MPP.

In 2008, Ding and Radhakrishnan [3] obtained a rigorous analytic solution for the optimum load (i.e., $R_{\rm opt} = V_{\rm mpp}/I_{\rm mpp}$) of an illuminated solar cell that contains a series resistance and a parallel conductance. This complex solution, which requires composite Lambert W functions, is important but it does not define the MPP. In 2015, Batzelis *et al*. [6] published approximate analytical expressions for the MPP using the Lambert W function. In 2017, Laudani *et al.* [7] obtained numerically the MPP by using bisection. In 2018, Wang *et al*. [9] presented approximate analytical expressions for MPP.

In this article, we present a simple procedure to calculate the MPP of illuminated PV panels or solar cells, using the single diode model. This rigorous procedure, which is based on fixed-point iteration, presents a robust convergence in only few iterations. In Section II, we review the fundamentals equations needed in the development of the algorithm. In Section III, we present the new algorithm and in Section IV, we compare it with the Newton–Raphson and bisection methods using measurements of PV modules with seven different technologies. We find that the new algorithm is simpler to implement and faster than the classical method of Newton–Raphson. In Section V, we compare the results of the first iterations of the present algorithm with previous approximate analytical solutions. We find that the fourth iteration of our algorithm is more accurate than that of the previous approximate analytical solutions.

II. Fundamental Equations

The *I–V* characteristics of illuminated PV panels are commonly described by the equivalent circuit of the single diode model presented in Fig. 1, which consists of a single exponential-type ideal junction, a constant photo-generated current source (I_{ph}), a series parasitic resistance (R_S), and a parallel parasitic conductance (G_p).

The mathematical description of this circuit is given by the following:

$$I = -I_o\left[\exp\left(\frac{V + I\,R_s}{n\,V_{th}}\right) - 1\right] - (V + I\,R_s)\,G_p + I_{ph} \tag{1}$$

where I is the terminal current, V is the terminal voltage, I_o is the reverse saturation current, n is the ideality factor multiplied for the number of cells connected in series, I_{ph} is the photo-generated current, and $V_{th} = {\rm k}T/{\rm q}$ is the thermal voltage. The previous implicit equation has the following solutions [1], [2], [5] for each variable I and V, as an explicit function of each other

Manuscript received June 15, 2020; revised July 29, 2020 and September 1, 2020; accepted September 3, 2020. Date of publication September 23, 2020; date of current version October 21, 2020. *(Corresponding authors: Orlando Trejo; Adelmo Ortiz-Conde.)*

The authors are with the Solid State Electronics Laboratory, Universidad Simón Bolívar, Caracas 1080, Venezuela (e-mail: orlandotrejo@ieee.org; ortizc@ieee.org).

Color versions of one or more of the figures in this article are available online at https://ieeexplore.ieee.org.

Digital Object Identifier 10.1109/JPHOTOV.2020.3022668

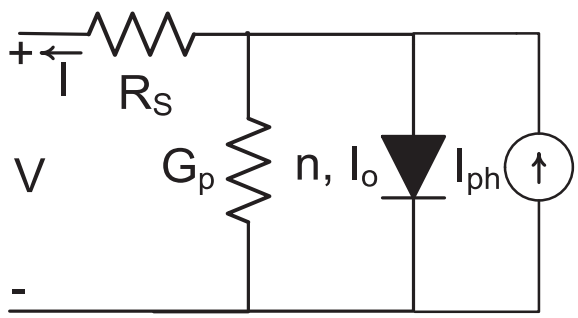

Fig. 1. Single diode model photovoltaic panel equivalent circuit including parasitic series resistance and parallel conductance.

and of the device model parameters:

$$I = -\frac{VG_P - (I_0 + I_{ph})}{1 + R_S\, G_P} - \frac{nV_{th}}{R_S}\,\mathrm{W}\left\{\frac{I_0 R_S}{nV_{th}\,(1 + R_S\, G_P)}\exp\left[\frac{V + R_S\,(I_0 + I_{ph})}{nV_{th}\,(1 + R_S\, G_P)}\right]\right\} \tag{2}$$

and

$$V = -I\left(R_S + \frac{1}{G_P}\right) + \frac{I_0 + I_{ph}}{G_P} - nV_{th}\mathrm{W}\left[\frac{I_0}{nV_{th}G_P}\exp\left(\frac{-I + I_0 + I_{ph}}{nV_{th}G_P}\right)\right] \tag{3}$$

where *W* represents the usual short-hand notation for the principal branch of the Lambert *W* function. This function, which is defined as the solution to the equation $W(x)\exp[W(x)] = x$, was first used in diode applications in 2000 [19], [20] and for solar cells in 2004 [1]. The rigorous short circuit current is obtained by evaluating (2) at $V = 0$

$$I_{SC} = +\frac{(I_0 + I_{ph})}{1 + R_S\, G_P} - \frac{nV_{th}}{R_S}\,\mathrm{W}\left\{\frac{I_0 R_S}{nV_{th}\,(1 + R_S\, G_P)}\exp\left[\frac{R_S\,(I_0 + I_{ph})}{nV_{th}\,(1 + R_S\, G_P)}\right]\right\} \tag{4}$$

which is typically approximated by $I_{SC} \cong I_{ph}$ when R_S and G_p are negligible. On the other hand, the open circuit voltage is evaluated using (3) with $I = 0$

$$V_{OC} = +\frac{I_0 + I_{ph}}{G_P} - nV_{th}\mathrm{W}\left[\frac{I_0}{nV_{th}G_P}\exp\left(\frac{I_0 + I_{ph}}{nV_{th}G_P}\right)\right] \tag{5}$$

which is approximated by $V_{OC} \cong nV_{th}\ln(I_{ph}/I_o)$ when G_p is negligible.

On the other hand, the power of the PV panel is

$$P = IV. \tag{6}$$

Tripathy *et al.* [8] in 2017 substituted (2) into (6) and obtained the power in terms of voltage

$$P = -\frac{V^2 G_P - V\,(I_0 + I_{ph})}{1 + R_S\, G_P} - \frac{VnV_{th}}{R_S}\,\mathrm{W}\left\{\frac{I_0 R_S}{nV_{th}(1 + R_S\, G_P)}\exp\left[\frac{V + R_S(I_0 + I_{ph})}{nV_{th}(1 + R_S\, G_P)}\right]\right\} \tag{7}$$

Then, taking the derivative of this equation with respect to voltage and equating it to zero, a transcendental equation is obtained which defines numerically the MPP

$$\frac{dP}{dV} = \{ -((1 + R_S\, G_P)\, nV_{th} + (1 + 2R_S\, G_P)\, V - (I_0 + I_{ph})\, R_S)\mathrm{W}\,[\alpha] - (2\, G_P V - I_0 - I_{ph})\, R_S - (1 + R_S\, G_P)nV_{th}\mathrm{W}^2[\alpha]\ \}/((1 + R_S\, G_P)\,(1 + \mathrm{W}[\alpha])R_S) \tag{8}$$

where

$$\alpha \equiv \frac{I_0 R_S}{(1 + R_S\, G_P)\, nV_{th}}\exp\left(\frac{(I_0 + I_{ph})\, R_S + V}{nV_{th}\,(1 + R_S\, G_P)}\right). \tag{9}$$

III. Fixed-Point Iteration Algorithm for the Maximum Power Point

We will now describe a new and simple procedure to calculate the MPP (V_{mpp}, I_{mpp}) based on the fixed-point iteration algorithm [21]. First, taking the derivative of (2) with respect to *V*, we obtain

$$\frac{dI}{dV} = -\frac{1}{R_S} + \frac{1}{R_S(1 + R_S\, G_P)} - \frac{W[x]}{R_S(1 + R_S\, G_P)(1 + W[x])} \tag{10}$$

where *x* is the following dimensionless intermediate variable used to obtain a compact notation

$$x \equiv \frac{I_0 R_S}{nV_{th}\,(1 + R_S\, G_P)}\exp\left[\frac{V + R_S\,(I_0 + I_{ph})}{nV_{th}\,(1 + R_S\, G_P)}\right]. \tag{11}$$

Noticing that *x* is also the argument in the Lambert W function in (2), we obtain *W*[*x*] from

$$\mathrm{W}\,[x] = -\frac{R_S I}{nV_{th}} - \frac{VG_P R_S - R_S\,(I_0 + I_{ph})}{nV_{th}\,(1 + R_S\, G_P)}. \tag{12}$$

Substituting (12) into (10), we obtain the derivative of *I* with respect to *V* in terms of *I* and *V*, without making use of any Lambert W function as (13), shown at the bottom of this page.

It is important to point out that the dynamic resistance of the device is -dV/dI and that (13) can also be obtained following a different approach [22]. Taking the derivative of the power in

$$\frac{dI}{dV} = -\frac{(1 + R_S\, G_P)\, I + G_P V - (G_P nV_{th} + I_0 + I_{ph})}{R_S\,(1 + R_S\, G_P)\, I + G_P R_S V - [(1 + R_S G_P)\, nV_{th} + R_S\,(I_0 + I_{ph})]}. \tag{13}$$

(6) with respect to V

$$\frac{dP}{dV} = I + V\frac{dI}{dV}. \tag{14}$$

Then, the MPP ($V_{\rm mpp}$, $I_{\rm mpp}$) is defined by the condition that dP/dV be zero. Substituting (13) into (14) and equating it to zero, we obtain

$$\begin{aligned}\frac{dP}{dV} = 0 = I_{\rm mpp} - V_{\rm mpp}\left\{\left(1 + R_S\, G_P\right) I_{\rm mpp} + G_P V_{\rm mpp}\right. \\ \left. - \left(G_P n V_{th} + I_0 + I_{ph}\right)\right\} / \left\{R_S\left(1 + R_S\, G_P\right) I_{\rm mpp}\right. \\ \left. + G_P R_S V_{\rm mpp} - \left[\left(1 + R_S G_P\right) n V_{th} + R_S\left(I_0 + I_{ph}\right)\right]\right\}.\end{aligned} \tag{15}$$

Rewriting the previous equation in a convenient quadratic form with respect to $I_{\rm mpp}$

$$0 = aI_{mpp}^2 + bI_{mpp} + c \tag{16}$$

where

$$a \equiv \left(1 + R_S\, G_P\right) R_S \tag{17}$$

$$b \equiv -\left(1 + R_S\, G_P\right) n V_{th} - R_S\left(I_0 + I_{ph}\right) - V_{\max} \tag{18}$$

and

$$c \equiv -G_P V_{\max}^2 + \left(G_P n V_{th} + I_0 + I_{ph}\right) V_{\max}. \tag{19}$$

Solving (16) and taking the appropriate root

$$I_{\rm mpp} = \frac{-b - \sqrt{b^2 - 4ac}}{2a} = -\frac{b}{2a} - \sqrt{\left(\frac{b}{2a}\right)^2 - \frac{c}{a}}. \tag{20}$$

It is worth mentioning that Laudani *et al.* [7] recently obtained an analogous quadratic equation of $V_{\rm mpp}$ in terms of $I_{\rm mpp}$ using a different approach. Rewriting (20) in order to show explicitly the dependence of $I_{\rm mpp}$ with respect to $V_{\rm mpp}$ as (21), shown at the bottom of this page

A second additional relationship between $I_{\rm mpp}$ and $V_{\rm mpp}$ is obtained by evaluating (3) at the MPP

$$\begin{aligned}V_{\rm mpp} = -I_{\rm mpp}\left(R_S + \frac{1}{G_P}\right) + \frac{I_0 + I_{ph}}{G_P} \\ - \; n V_{th} \mathrm{W}\left[\frac{I_0}{n V_{th} G_P} \exp\left(\frac{-I_{\rm mpp} + I_0 + I_{ph}}{n V_{th} G_P}\right)\right]\end{aligned} \tag{22}$$

If we substitute (22) into (21) we will obtain a rigorous equation with only one unknown variable (see Appendix)

$$I_{\rm mpp} = f\left(I_{\rm mpp}\right) \tag{23}$$

where f is a long function which contains the device parameters and only one variable $I_{\rm mpp}$. It is important to note that this equation is in the form of the classical fixed-point iteration algorithm [21], i.e., a given estimated value of $I_{\rm mpp}$ could be used in the right side of (23) in order to calculate an improved value of $I_{\rm mpp}$ in the left side of (23).

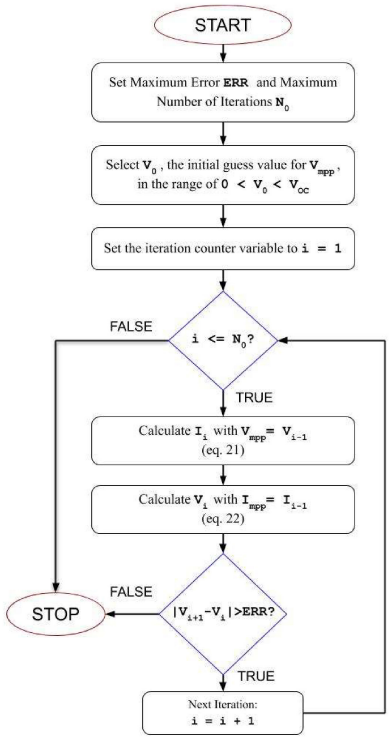

Fig. 2. Flowchart of present algorithm.

In order to avoid using the long f function in (23), we propose the following simple fixed-point iteration algorithm shown in Fig. 2. First, a maximum error (*ERR*) and a maximum number of iterations (N_0) are established. Second, an initial value of $V_{\rm mpp}$ (V_0) is selected in the range of $0 < V_0 < V_{OC}$. Third, the iteration is set to $i = 1$. Fourth, while $i < N_0$ the following steps are repeated. Fifth, we calculate I_i using (21) with $V_{\rm mpp} = V_{i\text{-}1}$. Sixth, we calculate V_i using (22) with $I_{\rm mpp} = I_i$. Seventh, if $|V_{i+1} - V_i| <$ ERR, the procedure is complete, otherwise the iteration is set to $i = i + 1$ and the procedure continues.

If the reader prefers to use the single long function $f\,(I_{\rm mpp})$, we recommend reading the Appendix. In the next section, we will demonstrate the robustness, accuracy, and fast convergence of this algorithm with measurements of different practical solar panels.

IV. Rigorous Calculation and Comparison With Newton–Raphson and Bisection Using Measurements of Various Technologies

Fig. 3 presents data from measurements done by the National Renewable Energy Laboratory (NREL) of PV modules with seven different technologies, in Cocoa Beach, Florida, on

$$I_{\rm mpp} = \frac{nV_{th}}{2R_S} + \frac{\left(I_0 + I_{ph}\right) R_S + V_{\rm mpp}}{2\left(1 + R_S\, G_P\right) R_S} - \sqrt{\left(\frac{nV_{th}}{2R_S} + \frac{\left(I_0 + I_{ph}\right) R_S + V_{\rm mpp}}{2\left(1 + R_S\, G_P\right) R_S}\right)^2 + \frac{G_P V_{\rm mpp}^2 - \left(G_P n V_{th} + I_0 + I_{ph}\right) V_{\rm mpp}}{\left(1 + R_S\, G_P\right) R_S}}. \tag{21}$$

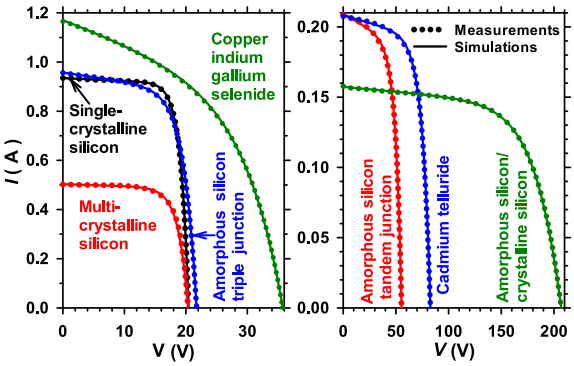

Fig. 3. Measurements and simulations with seven different technologies of PV module measured by NREL in Cocoa Beach on January 21, 2011 at 12:00 [23]. The parameters used for the simulations are presented in Table I.

TABLE I
EXTRACTED PARAMETERS FOR VARIOUS PHOTOVOLTAIC TECHNOLOGIES MEASURED BY NREL ON JANUARY 21, 2011 AT 12:00 [23]

TECHNOLOGY	nV_{th} (V)	I_o (nA)	I_{ph} (A)	R_S (mΩ)	G_p (mS)
Single-crystalline silicon	1.23	51.82	0.93	67.0	1.13
Multi-crystalline silicon	1.56	$1x10^3$	0.50	0.22	0.80
Cadmium telluride	7.64	$4x10^3$	0.21	0.58	0.21
Copper indium gallium selenide	6.27	$3x10^6$	1.17	0.15	9.53
Amorphous silicon/crystalline silicon	20.83	$7x10^3$	0.16	$3.08x10^4$	0.07
Amorphous silicon tandem junction	5.58	$9 x10^3$	0.21	0.69	0.43
Amorphous silicon triple junction	1.94	$1 x10^4$	0.96	$0.17x10^3$	3.77

January 21, 2011 at 12:00 [23]. These measurements consist of more than 100 nonuniformly spaced data range from ($V = 0$, $I = I_{SC}$) to ($V = V_{OC}$, $I = 0$). This figure also presents the simulations using the extracted parameters shown in Table I. We used the parameter extraction method presented in 2006 [2], which only requires a quadratic fit of the integration of the current with respect to the voltage. Hansen *et al.* [4] in 2013 used and improved this method. Since this extraction method is based on integrations, it needs uniformly spaced voltage data. Hence, we first interpolated the measured data in order to obtain 100 uniformly spaced points. Table II presents the corresponding MPP for the various PV technologies presented in Fig. 3. We compare the efficiency of the present method with respect to the classical Newton–Raphson method, the bisection method and the Maple function "fsolve" [24], using (8) which contains only one variable (V).

The implementation of the Newton–Raphson and the bisection method are well presented in [17]. All the calculations were done using a Maple environment with a portable computer with a 2.5 GHz i5-7300HQ microprocessor and 20 GB RAM. The initial value used for Newton–Raphson, "fsolve" and the present method was the 80% of the short circuit current ($I = 0.8I_{SC}$). On the other hand, for bisection the range of voltage was $0 < V < V_{OC}$.

TABLE II
MAXIMUM POWER POINT (V_{mpp}, I_{mpp}), OPEN CIRCUIT VOLTAGE (V_{oc}), AND SHORT CIRCUIT CURRENT (I_{sc}) FOR THE VARIOUS PHOTOVOLTAIC TECHNOLOGIES PRESENTED IN TABLE I

TECHNOLOGY	V_{mpp} (V)	I_{mpp} (A)	V_{OC} (V)	I_{SC} (A)
Single-crystalline silicon	17.05	0.85	20.43	0.93
Multi-crystalline silicon	16.57	0.45	20.44	0.5
Cadmium telluride	65.15	0.17	82.79	0.20
Copper indium gallium selenide	24.70	0.18	35.78	1.17
Amorphous silicon/crystalline silicon	157.49	0.17	206.87	0.16
Amorphous silicon tandem junction	42.89	0.18	55.37	0.21
Amorphous silicon triple junction	17.08	0.17	21.75	0.96

Since we are comparing seven different technologies, which present large variations in the ranges of currents and power and small variation in the ranges of voltages, it is more convenient to use the error in voltage. The maximum voltage error established for all methods was ERR $= 10^{-8}$ V. Table III presents the number of iterations and CPU time for the various methods and different technologies. We find that the smallest CPU time is obtained with the Maple function "fsolve" which does not give the number of iterations. On the other hand, the smallest number of iterations was obtained using the Newton–Raphson method. Our method is second best considering both the number of iterations and CPU time. We think that our method is better than Newton–Raphson in CPU time because Newton–Raphson is using classical (8) and our method is based on the combination of (21) and (22).

It is important to point out that all the methods converge for any initial value in the range of $0 < I < I_{SC}$ or $0 < V < V_{OC}$. In Section V, we compare previous approximate analytical equations for the MPP [6], [9] with the results of the first five iterations of the present method.

V. COMPARISON OF PREVIOUS APPROXIMATE EQUATIONS WITH THE FIRST FEW ITERATIONS OF THE PRESENT METHOD

In 2015, Batzelis *et al.* [6] proposed that the MPP ($V_{\rm mpp}$, $I_{\rm mpp}$) can be approximated by the following:

$$V_{\rm mpp} \approx (1 + R_S\, G_P)\, nV_{th} \left(\mathrm{W}\left[\frac{I_{ph}}{I_0} \exp(1) \right] - 1 \right) - R_S I_{ph} \left(1 - \frac{1}{\mathrm{W}\left[\frac{I_{ph}}{I_0} \exp(1) \right]} \right) \tag{24}$$

and

$$I_{\rm mpp} \approx + I_{ph} \left(1 - \frac{1}{\mathrm{W}\left[\frac{I_{ph}}{I_0} \exp(1) \right]} \right) - nV_{th} G_P \left(\mathrm{W}\left[\frac{I_{ph}}{I_0} \exp(1) \right] - 1 \right). \tag{25}$$

TABLE III
COMPARISON OF NUMBER OF ITERATIONS AND CPU TIME FOR VARIOUS NUMERICAL METHODS TO CALCULATE THE MAXIMUM POWER POINT USING DIFFERENT TECHNOLOGIES

TECHNOLOGY	NUMBER OF ITERATIONS			CPU TIME FOR 1000 CALCULATIONS (s)			
	PRESENT METHOD	NEWTON-RAPHSON	BISECTION	PRESENT METHOD	NEWTON-RAPHSON	BISECTION	MAPLE fsolve
Single-crystalline silicon	7	6	31	0.688	0.968	10.844	0.656
Multi-crystalline silicon	7	6	31	0.547	0.719	7.593	0.531
Cadmium telluride	6	5	33	0.610	0.765	11.19	0.547
Copper indium gallium selenide	6	6	32	0.578	0.984	11.094	0.829
Amorphous silicon/crystalline silicon	7	5	35	0.625	0.735	11.75	0.531
Amorphous silicon tandem junction	5	5	33	0.453	0.750	11.34	0.53
Amorphous silicon triple junction	6	5	32	0.578	0.750	10.88	0.59

TABLE IV
PERCENTAGE OF ABSOLUTE VOLTAGE ERRORS OF PREVIOUS APPROXIMATE EQUATION FOR THE MAXIMUM POWER POINT AND THE PRESENT METHOD USING FEW ITERATIONS FOR DIFFERENT TECHNOLOGIES

TECHNOLOGY	FIXED POINT ITERATIVE METHOD WITH:					BATZELIS	WANG
	1st ITERATION	2nd ITERATION	3rd ITERATION	4th ITERATION	5th ITERATION		
Single-crystalline silicon	11.93	7.12	0.33	$1.52\text{x}10^{-2}$	$7.03\text{x}10^{-4}$	0.24	0.53
Multi-crystalline silicon	8.48	6.91	0.40	$2.4\text{x}10^{-2}$	$1.41\text{x}10^{-3}$	0.47	0.63
Cadmium telluride	2.67	4.28	0.14	$4.99\text{x}10^{-3}$	$1.77\text{x}10^{-4}$	1.48	0.04
Copper indium gallium selenide	33.92	31.42	0.55	$2.04\text{x}10^{-2}$	$7.29\text{x}10^{-4}$	10.9	7.86
Amorphous silicon/crystalline silicon	1.93	3.10	0.14	$7.16\text{x}10^{-2}$	$3.5\text{x}10^{-4}$	1.25	0.44
Amorphous silicon tandem junction	1.23	1.97	$3.58\ \text{x}10^{-2}$	$7.14\text{x}10^{-4}$	$1.42\text{x}10^{-5}$	2.25	0.63
Amorphous silicon triple junction	2.48	4.28	0.12	$4.09\text{x}10^{-3}$	$1.32\text{x}10^{-4}$	1.34	0.05

On the other hand, in 2018 Wang *et al.* [9] presented the following approximations:

$$V_{\rm mpp} \approx nV_{th} \ln\left(\frac{I_{ph}}{I_0 \ln\left(\frac{I_{ph}}{I_0}\right)}\right) - R_S\left(I_{ph}+I_0\right) + \frac{R_S I_{ph}}{\ln\left(\frac{I_{ph}}{I_0}\right)} + nV_{th}G_P R_S \ln\left(\frac{I_{ph}}{I_0 \ln\left(\frac{I_{ph}}{I_0}\right)}\right) \quad (26)$$

and

$$I_{\rm mpp} \approx (I_{ph}+I_0) - \frac{I_{ph}}{\ln\left(\frac{I_{ph}}{I_0}\right)} - nV_{th}G_P \ln\left(\frac{I_{ph}}{I_0 \ln\left(\frac{I_{ph}}{I_0}\right)}\right). \quad (27)$$

These two previous approximated equations for the MPP will be compared with the first few iteration of the present method. The approximate analytical expressions present smaller CPU time but they are less accurate than the rigorous iterative solutions.

Table IV presents the percentage of absolute voltage errors of the first five iterations of the present method for various technologies. The percentage voltage error was calculated using $100*(V_{i+1}-V_i)/V_{i+1}$ where V_i and V_{i+1} *are* the obtained values of $V_{\rm mpp}$ for the $i+1$ and the i iterations. The initial value used was the 80% of the short circuit current ($I = 0.8I_{SC}$). This table also shows the corresponding results obtained using the previous approximate equations. We see in this table that the fourth iteration of our method is better than the approximate equations of Batzelis *et al.* [6] and Wang *et al.* [9] and for all the technologies analyzed. On the other hand, the third iteration of our method is comparable to the previous approximate equations.

VI. CONCLUSION

We have presented a simple algorithm to calculate the MPP of illuminated PV panels based on the algorithm of fixed-point iteration. This simple and rigorous procedure presents a fast convergence for any initial value. This algorithm does not require the evaluation of derivatives in contrast with the classical method of Newton–Raphson. Our algorithm has been tested with simulated data using the extracted parameters of seven different technologies of PV panel measured by the NREL in Cocoa Beach, Florida. For convenience, the error in voltage is used in order to compare the different PV technologies, which present larger

variations in the range of currents and power. Our calculations indicate that the present algorithm requires less CPU time than the classical methods of Newton–Raphson and bisection. We have also compared our algorithm with previously developed approximate solutions and we conclude that the fourth iteration is more accurate than the previous analytical approximations for the MPP.

APPENDIX

In what follows, we will study the convergence of the present algorithm. Substituting (22) into (21) we obtain a long rigorous equation with only one unknown variable

$$I_{\rm mpp} = f\left(I_{\rm mpp}\right) = + \left(I_2 - c_3 I_{\rm mpp} - I_9 \mathrm{W}\left[c_1 \exp\left(-\frac{I_{\rm mpp}}{I_1}\right) + c_2\right] + I_3\right) - \left\{ \left(I_2 - c_3 I_{\rm mpp} - I_9 \mathrm{W}\left[c_1 \exp\left(-\frac{I_{\rm mpp}}{I_1}\right) + c_2\right] + I_3\right)^2 + \left(I_4 - c_4 I_{\rm mpp} - I_5 \mathrm{W}\left[c_1 \exp\left(-\frac{I_{\rm mpp}}{I_1}\right) + c_2\right]\right)^2 - \left(I_6^2 - I_7 I_{\rm mpp} - I_8^2 \mathrm{W}\left[c_1 \exp\left(-\frac{I_{\rm mpp}}{I_1}\right) + c_2\right]\right) \right\}^{1/2} \quad \text{(A1)}$$

where I_1 to I_9 are constants with units of current, $I_1 \equiv G_P n V_{th}$, $I_2 \equiv \frac{I_0+I_{ph}}{2(1+R_S G_P)R_S G_P}$, $I_3 \equiv \frac{nV_{th}}{2R_S} + \frac{I_0+I_{ph}}{2(1+R_S G_P)}$, $I_4 \equiv \frac{I_0+I_{ph}}{(R_S G_P(1+R_S G_P))^{1/2}}$, $I_5 \equiv (\frac{G_P}{(1+R_S G_P)R_S})^{1/2} n V_{th}$, $I_6 \equiv (\frac{(G_P n V_{th}+I_0+I_{ph})(I_0+I_{ph})}{(1+R_S G_P)R_S G_P})^{1/2}$, $I_7 \equiv \frac{(G_P n V_{th}+I_0+I_{ph})(R_S+G_P^{-1})}{(1+R_S G_P)R_S}$, $I_8 \equiv (\frac{(G_P n V_{th}+I_0+I_{ph})n V_{th}}{(1+R_S G_P)R_S})^{1/2}$, $I_9 \equiv \frac{nV_{th}}{2(1+R_S G_P)R_S}$ and c_1 to c_4 are dimensionless constants, $c_1 \equiv \frac{I_0}{G_P n V_{th}}$, $c_2 \equiv \frac{I_0+I_{ph}}{G_P n V_{th}}$, $c_3 \equiv \frac{1}{2G_P R_S}$ and $c_4 \equiv (1+\frac{1}{R_S G_P})^{1/2}$.

According to [21, Th. 2.4], the fixed-point iteration method, $I_{\rm mpp} = f(I_{\rm mpp})$, will always converge in a range $I_{\rm low} < I_{\rm mpp} < I_{\rm high}$ if the following condition is satisfied:

$$\left|\frac{df}{dI_{\rm mpp}}\right| < 1. \quad \text{(A2)}$$

It is important to point out that convergence could also occur for the cases in which the condition (A2) is not satisfied.

Fig. 4 shows the normalized function $f(I)/I_{SC}$, obtained from the evaluation of (A1), as a function of the normalized current $f(I)/I_{SC}$ for seven different technologies of PV module measured by NREL in Cocoa Beach [23]. The parameters used for the simulations are presented in Table I. This figure also presents the corresponding derivative of $f(I)$ with respect to the current. We observe that the magnitude of derivative of $f(I)$ is greater than 1 only for values approaching I_{SC}. Therefore, condition (A2) implies that there is always convergence for all values of current except when it approaches to I_{SC}. It is worth noticing that this condition does not imply that it will diverge when the initial current approaches I_{SC}.

We tested many cases using initial values greater than I_{SC} and we always found convergence. The left side of Fig. 5 presents

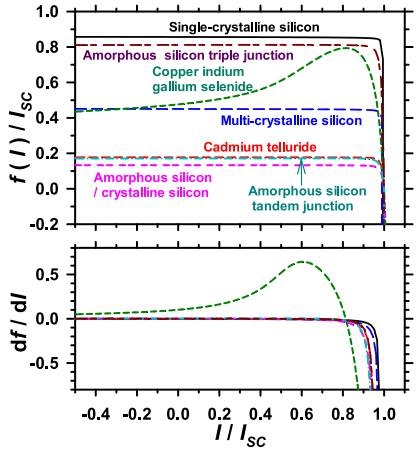

Fig. 4. Function $f(I)$, normalized with respect to I_{SC}, obtain from the evaluation of (A1), as a function of the normalized current for seven different technologies of PV module measured by NREL in Cocoa Beach [23] (top). The corresponding derivative of $f(I)$ with respect to the current as a function of the normalized current (bottom).

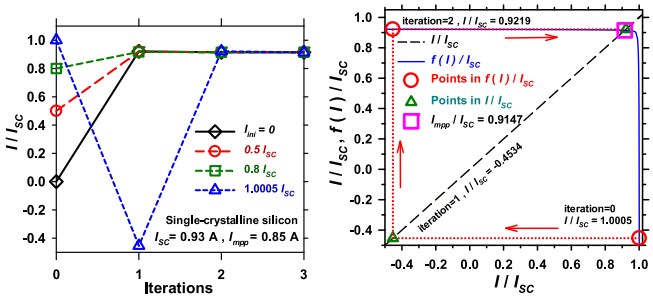

Fig. 5. Normalized current (I/I_{SC}) as a function of the number of iterations (left). The selected initial values (i.e., iteration = 0) of normalized current are: 0, 0.5, 0.8, and 1.0005. Graphical solution for the case of $I/I_{SC} = 1.0005$ (right). The blue solid and the dashed black lines illustrate $f(I)/I_{SC}$ and the straight line I/I_{SC} respectively. The interception of both plots is the solution, defined by (A1), and is shown as a pink square. The red circles and the green triangles show the iteration values in $f(I)/I_{SC}$ and the straight line I/I_{SC}. The red dotted line indicates the trajectory of the iterations.

the normalized current (I/I_{SC}) as a function of the number of iterations for the single-crystalline silicon case. The selected initial values (i.e., iteration = 0) of normalized current are: 0, 0.5, 0.8, and 1.0005. We see in this figure that for initial values $I/I_{SC} \leq 0.8$, the convergence requires practically one iteration and that for the case $I/I_{SC} = 1.0005$ the convergence needs only two iterations. The case of $I/I_{SC} = 1.0005$ presents a very interesting behavior when it goes to a negative value of -0.45 in the first iteration and 0.92 in the second iteration. The case of $I/I_{SC} = 2$ also converges but it is not illustrated in the figure because it will be out of scale since it goes to -13189, -0.036, and $+0.92$ in first three iterations.

The right side of Fig. 5 presents a graphical solution for the case of $I/I_{SC} = 1.0005$. The solid line illustrates $f(I)/I_{SC}$, the dashed line corresponds to I/I_{SC}, and the interception is the solution defined by (A1). First, the evaluation of $f(I)/I_{SC}$ at the initial value of 1.0005 (i.e., iteration = 0) gives -0.4534 which is shown with a red circle. Second, the evaluation of $f(I)$ at the value

of -0.4534 (iteration = 1) gives 0.9219. Third, the evaluation of $f(I)$ at the value of 0.9219 (iteration = 3) gives 0.9144 which is very close to the solution of 0.9147. This graphical procedure indicates that there will always be convergence if $f(I)$ presents a behavior similar to the curves of Fig. 4. Based on all the cases we have tested, we conclude that our method converges for any initial value of current.

ACKNOWLEDGMENT

The authors would like to thank Dr. B. Marion and his coworkers from the NREL, for the comprehensive measured data of PV modules which is in public domain. They also would like to thank the reviewers and the editor for their valuable work which has led to a significant improvement in the quality of this article.

REFERENCES

[1] A. Jain and A. Kapoor, "Exact analytical solutions of the parameters of real solar cells using Lambert W-function," *Sol. Energy Mater. Sol. Cells*, vol. 81, pp. 269–277, 2004.

[2] A. Ortiz-Conde, F. J. García Sánchez, and J. Muci, "New method to extract the model parameters of solar cells from the explicit analytic solutions of their illuminated *I-V* characteristics," *Sol. Energy Mater. Sol. Cells*, vol. 90, pp. 352–361, Feb. 2006.

[3] J. Ding and R. Radhakrishnan, "A new method to determine the optimum load of a real solar cell using the Lambert W-function," *Sol. Energy Mat. Sol. Cells*, vol. 92, no. 12, pp. 1566–1569, 2008.

[4] C. W. Hansen, A. Luketa-Hanlin, and J. S. Stein, "Sensitivity of single diode models for photovoltaic modules to method used for parameter estimation," in *Proc. 28th Eur. PV Sol. Energy Conf.*, Paris, France, Sep./Oct. 2013, pp. 3258–3264.

[5] A. Ortiz-Conde, F. J. García-Sánchez, J. Muci, and A. Sucre-González, "A review of diode and solar cell equivalent circuit model lumped parameter extraction procedures," *Facta Universitatis-Ser., Electron. Energetics*, vol. 27, no. 1, pp. 57–102, Mar. 2014.

[6] E. I. Batzelis, G. E. Kampitsis, S. A. Papathanassiou, and S. N. Manias, "Direct MPP calculation in terms of the single-diode PV model parameters," *IEEE Trans. Energy Convers.*, vol. 30, no. 1, pp. 226–236, Mar. 2015.

[7] A. Laudani *et al.*, "An analytical approach for maximum power point calculation for photovoltaic system," in *Proc. Eur. Conf. Circuit Theory Des.*, 2017, pp. 1–4.

[8] M. Tripathy, M. Kumar, and P. K. Sadhu, "Photovoltaic system using Lambert W function-based technique," *Sol. Energy*, vol. 158, pp. 432–439, 2017.

[9] S.-N. Wang, Q.-G. Chen, and W.-G. Gao, "An improved analytical solution for MPP parameters of photovoltaic cells," *Sol. Energy*, vol. 174, pp. 848–854, 2014.

[10] C. B. Jones and C. W. Hansen, "Single diode parameter extraction from in-field photovoltaic I-V curves on a single board computer," in *Proc. IEEE Photovolt. Specialists Conf.*, 2019, vol. 8981330, pp. 382–387.

[11] A. Dehghanzadeh, G. Farahani, and M. Maboodi,, "A novel approximate explicit double-diode model of solar cells for use in simulation studies," *Renewable Energy*, vol. 103, pp. 468–477, 2017.

[12] X. Gao *et al.*, "Lambert W-function based exact representation for double diode model of solar cells: Comparison on fitness and parameter extraction," *Energy Convers. Manage.*, vol. 127, pp. 443–460, Nov. 2016.

[13] C. Chellaswamy *et al.*, "A novel optimization method for parameter extraction of industrial solar cells," in *Proc. Innov. Power Adv. Comput. Technol.*, 2019, pp. 1–6.

[14] A. Ortiz-Conde, D. Lugo-Muñoz, and F. J. G. Sánchez, "An explicit multiexponential model as an alternative to traditional solar cell models with series and shunt resistances," *IEEE J. Photovolt.*, vol. 2, no. 3, pp. 261–268, Jul. 2012.

[15] E. M. Vicente, P. D. Santos Vicente, R. L. Moreno, and E. R. Ribeiro, "High-efficiency MPPT method based on irradiance and temperature measurements," *IET Renewable Power Gener.*, vol. 14, pp. 986–995, 2020.

[16] J.-S. Ko, J.-H. Huh, and J.-C. Kim, "Overview of maximum power point tracking methods for PV system in micro grid," *Electron.*, vol. 9, 2020, Art. no. 816.

[17] S. Chun and A. Kwasinski, "Analysis of classical root-finding methods applied to digital maximum power point tracking for sustainable photovoltaic energy generation," *IEEE Trans. Power Electron.*, vol. 26, no. 12, pp. 3730–3743, Dec. 2011.

[18] M. Louzazni, A. Khouya, S. Al-Dahidi, M. Mussetta, and K. Amechnoue, "Analytical optimization of photovoltaic output with Lagrange multiplier method," *Optik*, vol. 199, 2019, Art. no. 163379.

[19] T. C. Banwell and A. Jayakumar, "Exact analytical solution for the current flow through diode with series resistance," *Electron. Lett.*, vol. 36, no. 4, pp. 291–292, 2000.

[20] A. Ortiz-Conde, F. J. García Sánchez, and J. Muci, "Exact analytical solutions of the forward non-ideal diode equation with series and shunt parasitic resistances," *Solid-State Electron.*, vol. 44, pp. 1861–1864, Oct. 2000.

[21] R. L. Burden, J. D. Faires, and A. C. Reynolds, *Numerical Analysis*, 2nd ed. Boston, MA, USA: Prindle, Weber & Schmidt, 1981.

[22] F. J. García-Sánchez, "Understanding photovoltaic cell dynamic resistance behavior with changing incident light intensity," 2019, *techrxiv.11295065.v1*.

[23] B. Marion *et al.*, "New data set for validating PV module performance models," in *Proc. IEEE 40th Photovolt. Specialist Conf.*, 2014, pp. 1362–1366.

[24] Maplesoft. Waterloo Maple Inc., Waterloo, ON, Canada. (2014). [Online]. Available: http://www.maplesoft.com